CHEMISTRY
A EUROPEAN JOURNAL

DOI: 10.1002/chem.200900995

A Complete Multiscale Modelling Approach for Polymer–Clay Nanocomposites

Giulio Scocchi,[a, c] Paola Posocco,*[a] Jan-Willem Handgraaf,[b] Johannes G. E. M. Fraaije,[b, d] Maurizio Fermeglia,[a] and Sabrina Pricl[a]

Abstract: We present an innovative, multiscale computational approach to probe the behaviour of polymer–clay nanocomposites (PCNs). Our modeling recipe is based on 1) quantum/force-field-based atomistic simulation to derive interaction energies among all system components; 2) mapping of these values onto mesoscopic bead–field (MBF) hybrid-method parameters; 3) mesoscopic simulations to determine system density distributions and morphologies (i.e., intercalated versus exfoliated); and 4) simulations at finite-element levels to calculate the relative macroscopic properties. The entire computational procedure has been applied to two well-known PCN systems, namely Nylon 6/Cloisite 20A and Nylon 6/Cloisite 30B, as test materials, and their mechanical properties were predicted in excellent agreement with the available experimental data. Importantly, our methodology is a truly bottom-up approach, and no "learning from experiment" was needed in any step of the entire procedure.

Keywords: bead–field hybrid simulation · materials science · molecular modeling · nanostructures · organic–inorganic hybrid composites

Introduction

In recent years major scientific efforts have been devoted to the possibility of using layered silicate (LS) nanoparticles as fillers for novel structural and functional polymer materials.[1] This interest stems from many factors, above all the abundant availability of the clay materials and the lack of health hazards of these nanoparticles when compared to prefabricated needle- and whisker-shaped ones. Moreover, due to their high aspect ratio, the addition of very low volume fractions of LS nanoparticles allows improvements in material properties comparable to those of traditional fillers, and can even result in completely new features for the polymer matrix. Finally, the possibility of using standard synthetic routes (e.g., melt intercalation techniques) to produce these nanocomposites makes them extremely appealing also from the economical standpoint. Indeed, many efforts are currently being made in both industry and academia worldwide in the development of nanocomposites with applications ranging from lightweight automotive engineering plastics with increased stiffness/toughness performance and higher heat distortion temperature, to reinforced transparent glasses, barrier resins, low-stress advanced structural materials, halogen-free flame-retardant coatings, polyelectrolyte membranes for fuel cells and batteries, and even novel light-emitting diodes.[1,2]

Depending on the nature of the components used and the method of preparation, three main types of composites can be obtained with layered silicate materials. When the polymer is unable to intercalate (or penetrate) between the silicate sheets, a phase-separated composite is obtained, and the properties remain in the same range as those for traditional microcomposites. In an intercalated structure, in which polymer chains can penetrate between the silicate

[a] Dr. G. Scocchi,[+] P. Posocco,[+] Prof. M. Fermeglia, Prof. S. Pricl
Molecular Simulation Engineering (MOSE) Laboratory, DICAMP
University of Trieste, Piazzale Europa 1, 34127 Trieste (Italy)
Fax: +(39)-040569823
E-mail: paola.posocco@dicamp.units.it
Homepage: http://www.mose.units.it

[b] Dr. J.-W. Handgraaf, Prof. J. G. E. M. Fraaije
CULGI B.V., P.O. Box 252, 2300 AG Leiden (The Netherlands)

[c] Dr. G. Scocchi[+]
Presently at the University for Applied Sciences
of Southern Switzerland (SUPSI)
Institute of Computer Integrated Manufacturing
for Sustainable Innovation (ICIMSI)
Centro Galleria 2, CH-6928 Manno (Switzerland)

[d] Prof. J. G. E. M. Fraaije
Leiden Institute of Chemistry, Soft Matter Chemistry
Gorlaeus Laboratories, Universiteit Leiden
Einsteinweg 55, 2333 CC Leiden (The Netherlands)

[+] These authors equally contributed to this work.

Supporting information for this article is available on the WWW under http://dx.doi.org/10.1002/chem.200900995.

layers, a well-ordered multilayer morphology results with alternating polymer and inorganic layers. When the silicate layers are completely and uniformly dispersed in a continuous polymer matrix, an exfoliated or delaminated structure is obtained. In each case, the physical properties of the resultant composite are significantly different.

Fabricating polymer clay nanocomposites (PCNs) in an efficient and cost-effective manner, however, poses significant synthetic challenges, which can be appreciated by considering the structure of the clay particles. The layered silicates commonly used in nanocomposites, of which montmorillonite (MMT) is a prime example, belong to the structural family known as the 2:1 phyllosilicates. Their crystal lattice consists of two-dimensional layers in which a central octahedral sheet of alumina or magnesia is fused between two external silica tetrahedrons by the tips, so that the oxygen ions of the octahedral sheet also belong to the tetrahedral sheets (Figure 1a). These layers organize themselves to form stacks with a regular van der Waals gap in between them, called the interlayer region or gallery. Isomorphic substitution of some elements within the layers (e.g., Al^{3+} by Mg^{2+}, or Mg^{2+} by K^{+}) generates negative charges that are counterbalanced by alkali or alkaline earth metal cations situated in the interlayers. The lateral dimensions of these layers can vary from approximately 200 Å to several micrometers, depending on the particular composition of the silicate, while the spacing between the closely packed sheets is on the order of 1 nm, which is smaller than the radius of gyration of typical polymers (Figure 1b). Consequently, there is a large entropic barrier that inhibits the polymer's penetrating this gap and becoming intermixed with the clay.

To enhance polymer–clay interaction, a cation-exchange process is employed in which hydrophilic cations (e.g., Na^{+} or K^{+}) are exchanged by a surface modifier, usually selected from a group of organic substances having at least one alkyl group, most commonly quaternary ammonium salts (quats; Figure 1c). The role of this organic component in organosilicates is to lower the surface energy of the inorganic host and improve the wetting characteristic with the polymer. Intuitively, the nature and the structure of these "compatibilisers" determines the hydrophobicity of the silicate layers and hence their extent of exfoliation (Figure 1d).

Although several issues must be addressed to optimise the production of PCN materials, of foremost importance is

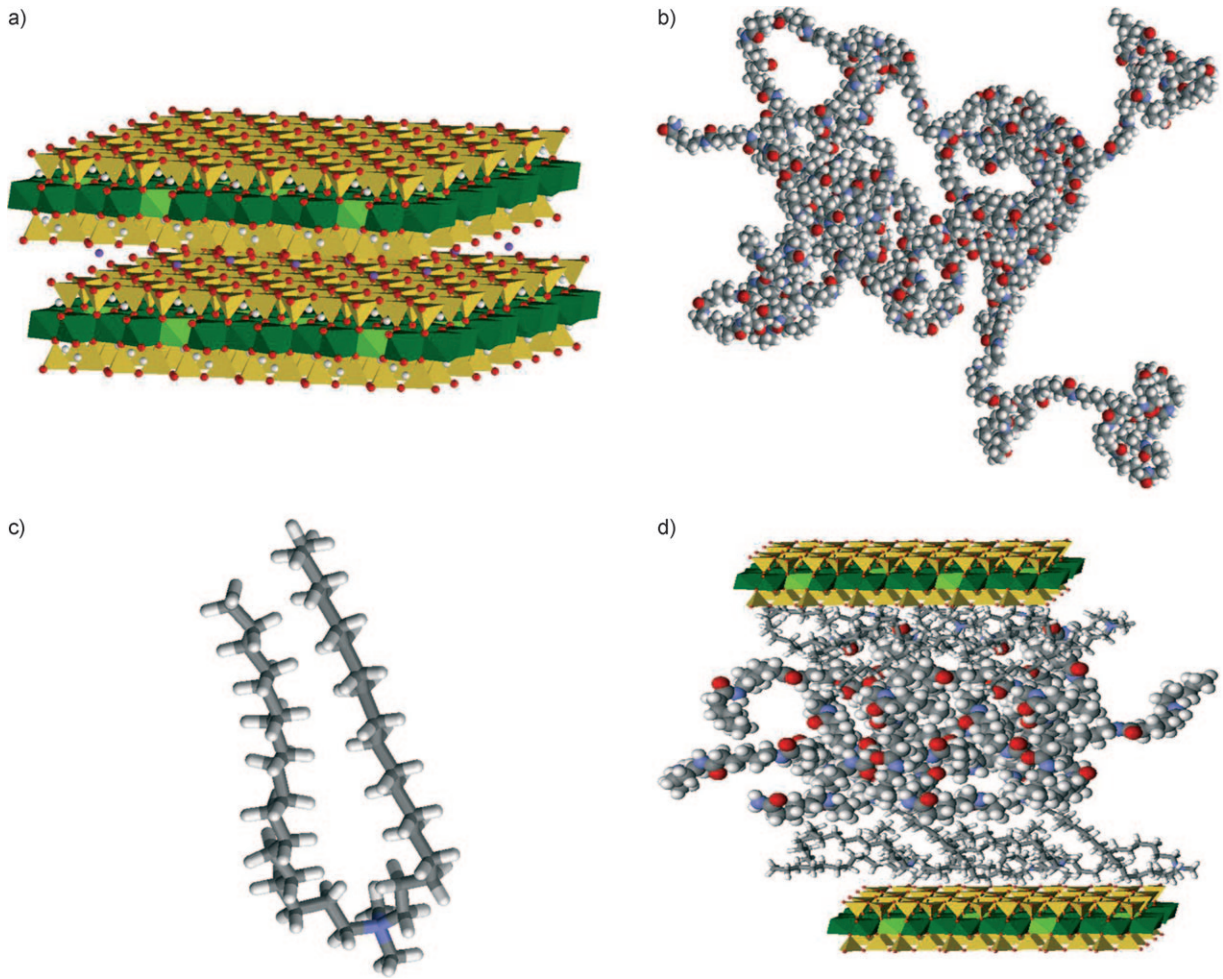

Figure 1. a) Silicate layers commonly used in PCNs. b) Single polymer chain. c) Molecular structure of an alkyl cationic surface modifier. d) Example of a typical PCN system after intercalation. Color code: H white, O red, N blue, Si yellow, Al dark green, Mg light green.

to identify conditions that promote penetration of the polymer into the narrow clay galleries. However, if the mineral sheets ultimately phase-separate from the polymeric matrix, the mixture will not exhibit improved strength, heat resistance, or barrier properties. Therefore, it is also essential to determine the factors that control the macroscopic phase behaviour of the mixture. Finally, the properties of the hybrid system commonly depend on the structure of the material; thus, it is of particular interest to establish the morphology of the final composite.

A current challenge of physical, chemical, and engineering sciences is to develop theoretical tools for predicting structure and physical properties of PCNs from knowledge of a few input parameters.[3] However, despite all efforts, progress in the prediction of macroscopic physical properties from structure has been slow. Major difficulties are related to the fact that 1) the microstructural elements in multiphase materials are not shaped or oriented as in the idealizations of computer simulations, and more than one type can coexist; 2) multiple length and timescales are generally involved and must be taken into account when overall thermodynamic and mechanical properties are to be determined; and 3) the effect of the interphases and/or interfaces on the physical properties is often not well understood and characterized. As a consequence, their role is often neglected in the development of new theoretical tools or they are treated in a very empirical way. In this work, we focus on the understanding and efficient treatment of issues 2 and 3) in a multiscale molecular simulation framework, with the ultimate goal of developing a computationally based nanocomposite design tool.

Currently, atomistic level simulations such as molecular dynamics (MD) and Monte Carlo (MC) techniques allow structure and properties to be predicted for systems with large numbers of atoms and timescales on the order of microseconds. Although this can lead to many relevant results in material design, many critical phenomena in this field still require timescales and length scales far too large for practical MD/MC simulations. Therefore, we need to develop methods treating the mesoscale (MS), which sets in between the atomistic length and timescales of MD/MC and the macroscopic length and timescales (micro- to millimeter, and microseconds to seconds) pertinent, for instance, to finite-element (FE) analysis. This linking through the mesoscale is probably the greatest challenge for developing reliable first-principles methods for practical and effective material design. Given these concepts, it is also necessary to carry out calculations for realistic length/time scales fast enough to be practically useful in materials design. This requires developing techniques functional for engineers, by incorporating the methods and results obtained at smaller scales (e.g., MD) into MS simulations, and the morphologies thus predicted into FE calculations. Accordingly, we developed a hierarchical procedure for bridging the gap between atomistic and FE calculations for PCN design. The mesoscopic bead–field (MBF)[4] hybrid method was adopted as the simulation technique, and all necessary parameters of the mesoscopic model are estimated by a step-by-step procedure involving 1) matching of the atomistic and mesoscopic pair-correlation functions to determine the best mesoscopic topology for the organic modifiers, 2) mapping of interaction energies obtained from atomistic simulations onto the mesoscopic bead–bead interaction parameters, and 3) matching the atomistic and polymer density profiles. Finally, the mesoscopic simulated structures are passed on to the FEM calculations, to estimate macroscopic properties of the PCN such as Young's modulus.

Results and Discussion

The multiscale molecular modeling strategy developed in this work to obtain some industrially relevant macroscopic properties of polymer clay nanocomposites relied on several consecutive steps, which are summarized in Scheme 1.

1. Generate and optimize clay, polymer and compatibilizer 3D atomistic models (**QM,MD**)
2. Generate atom-based pair correlation functions for the compatibilizer (**MD**); **3.** Generate soft-core pair correlation functions for the compatibilizer (**BD**); **4.** Map soft-core pair correlations onto atom-based pair correlation functions of compatibilizer
5. Calculate (**MD**) and scale binding energies from the atomistic simulations of step **1**; **6.** Map the scaled binding energies to soft-core interaction parameters
7. Generate atom-based density profile for the polymer (**MD**); **8.** Generate density profiles for polymer field model (**MBF**); **9.** Map field density profile onto atom-based density profile of polymer
10. Obtain system structure with the parameter sets determined from step **1** to **9** (**MBF**)
11. Import the obtained structure and perform a simulation to estimate the macroscopical properties of the system (**FE**)
12. If the required material performances are achieved, then stop, else restart from step **1** by changing one or more system components

Scheme 1. Multiscale computational recipe for characterizing a novel PCN for a given application. Where applicable the used simulation method is given in parentheses. **QM**, quantum mechanics; **MD**, molecular dynamics; **BD**, Brownian dynamics; **MBF**, mesoscopic bead–field hybrid method; **FE**, finite-element method.

After building and optimizing the three-dimensional models of each PCN system component (i.e., MMT, polymer, and surface compatibiliser or quat) (Scheme 1, step 1), matching of the atomistic and mesoscopic pair correlation functions for the quats, obtained from atomistic MD and mesoscopic BD simulations, respectively, was performed to determine the best mesoscopic topology for the organic modifiers (Figure 2; Scheme 1, steps 2–4).

The mesoscopic nanocomposite models resulting from the mapping procedures contained four different species of beads: one for the polymer chain (P), two for the quat (H for the polar head and T for the apolar tails), and one for the MMT surface (M). The nonbonded interaction energies among the PCN components, calculated by atomistic MD simulations and rescaled by a combinatorial method which accounts for the number of contacts between n_i particles of type i and n_j particles of type j, led to the mesoscopic interaction parameters listed in Table 1 (Scheme 1, steps 5–9).

According to the recipe, the corresponding MBF hybrid simulations were then performed, and the relevant meso-

Table 1. Mesoscopic interaction parameters for the two PCN systems considered.[a] Top set of values: MMT/Nylon6 $M_2(C_{18})_2$; bottom set of values: MMT/Nylon6 M_3C_{18}.

a_{ij}	H	M	T
H	496.3	5	37.8
M	5	15	32.5
T	37.8	32.5	32
c_{ij}	H	M	T
P	5	5	10
a_{ij}	H	M	T
H	500	5	30.9
M	5	15	30.6
T	30.9	30.6	31.8
c_{ij}	H	M	T
P	5	5.5	9.5

[a] Mesoscopic bead types: P = polymer bead; H = quat polar head bead; T = quat apolar tail bead; M = montmorillonite bead.

scale morphologies of the systems were obtained. Figure 3 illustrates the MBF simulation results obtained for one of the two Nylon 6/MMT nanocomposites considered. The compatibiliser chosen here was a dimethyl dioctadecyl quaternary ammonium chloride (M_3C_{18}), in line with the idea of modeling a commercial surfactant (Cloisite 20A; see Scheme 1, step **10**). The predicted morphology compares well with recent TEM images of Nylon 6 nanocomposites:[5] a fixed wall of nanoclay is obtained, to which the polar heads of the surfactant molecules are attracted to and onto which the long, apolar hydrocarbon surfactant tail is flattened. The charged parts of the surfactant remain close to the MMT layers, leaving the tails of the organic molecules

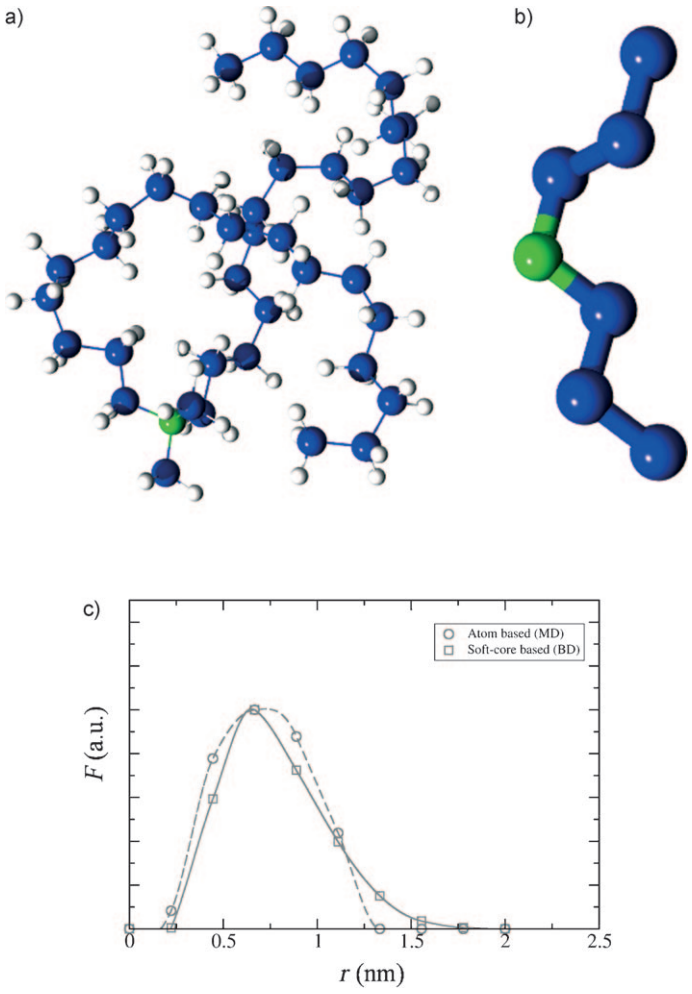

Figure 2. Mapping of alkyl cationic surface modifier. a) Snapshot of atomistic structure. b) Snapshot of optimal mesoscopic structure containing one head bead and three beads per tail. c) Typical mapping of a pair correlation function of the atomistic model and the mesoscopic model.

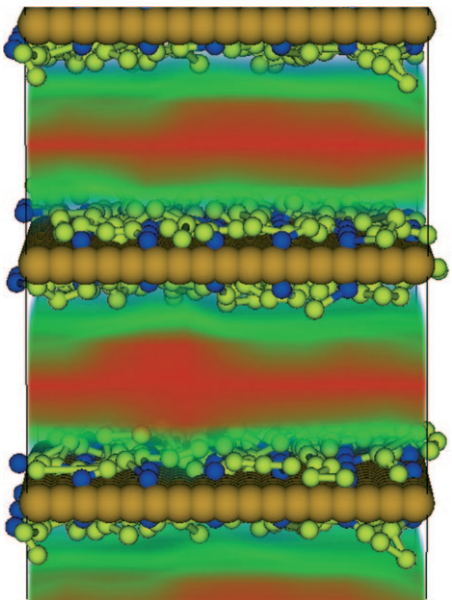

Figure 3. Snapshot of the structure of PCN obtained with the MBF hybrid simulation method. The clay platelets and compatibiliser molecules are represented in the method as soft-core beads, and the polymer is represented by a field model. Bead color code: brown, clay bead; blue/light green, compatibiliser. Field color code: red, high density values; green, intermediate density values; blue, low density values.

to interact with the Nylon 6 chains. However, areas are available on the clay surface for entering into contact with the polymer, and thus the effective binding between the components of the nanosystem is rendered almost ideal.

The mesoscale morphologies thus obtained were used as input for a finite-element (FE) analysis to estimate the value of the Young's modulus of intercalated stacks and, subsequently, of the relevant composite (Scheme 1, step **11**). Figure 4a shows a cut plane of the reference cell (Figure 4b) implemented in the calculations.

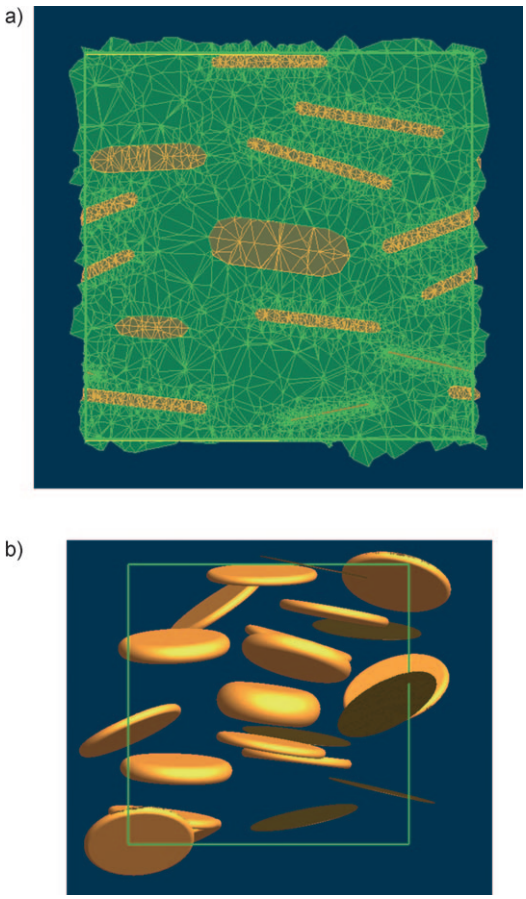

Figure 4. a) Cut plane of reference cell b) for the FE calculation. Clay layers embedded in the matrix are colored in orange. In the reference cell b), the polymer is omitted for clarity.

The FE calculations of the Young's modulus E yielded results which are in excellent agreement with the corresponding experimental data. Indeed, the predicted value of $E=$ 4.19 GPa for the Nylon 6/MMT PCN with M_3C_{18} as compatibiliser compares well to the experimental value of 4.32 GPa.[5] Applying the same procedure to the Nylon 6/MMT nanocomposite with $M_2(C_{18})_2$ as quat gave analogous quantitative results ($E_{calcd}=4.41$, $E_{exptl}=4.60$ GPa).[5] The estimated value for the nanocomposite with M_3C_{18} as quat is higher than that of the PCN with $M_2(C_{18})_2$, in harmony with the different degrees of exfoliation that were modelled. Discrepancies between predicted and measured quantities could be due, for instance, to a different degree of crystallinity or different crystalline forms of Nylon 6 in the presence of MMT nanofillers, as claimed by some authors.[6]

Conclusions

There are many levels at which molecular modeling and simulation can be useful, ranging from the highly detailed ab initio quantum mechanics, through classical, atomistic molecular modeling, to process engineering modeling. These computations can significantly reduce the need for experiments, allow products and processes to be optimized and permit large numbers of candidate materials to be screened prior to production. These techniques are currently used to obtain thermodynamic information about pure or mixed systems. Properties obtained using these microscopic properties assume the system to be homogeneous in composition, structure and density, which is clearly a limitation. When a system is complex, comprizing several components, which may sparingly miscible, of which PCNs are prime examples, peculiar phases with remarkable properties can be observed. These so-called mesophases comprise far too many atoms for description by atomistic modeling. Hence, coarse-grained methods are better suited to simulate such structures.

One of the primary techniques for mesoscale simulation is the mesoscopic bead–field (MBF) hybrid method,[4] an innovative technique in which beads and fields are both part of the same simulation. However, retrieving information on mesophase structures is not enough for predicting macroscopic features of such materials. This is possible if mesophase modeling is coupled with appropriate finite-element tools that, provided properties of pure components are given or can be in turn obtained by simulation, allows a realistic estimation of many nanocomposite features to be obtained.

The global perspective of our work is the complete integration of all available simulation scales, in a hierarchical procedure, to provide an efficient and robust simulation protocol for the successful design of PCNs of industrial interest and predict their final performance. Although the proposed computational recipe could still be refined by considering, for instance, the a priori definition of platelet spatial distribution and a more precise analysis of different morphologies (issues that are currently being addressed by us), to our knowledge this is the first successful computational procedure able to predict, with a high degree of confidence, hierarchical structures and behaviour of PCNs, and to capture all the phenomena taking place on length scales that typically span 5–6 orders of magnitudes and timescales encompassing a dozen of orders of magnitude.

Experimental Section

The entire modeling recipe is based on 1) quantum/molecular mechanics-based atomistic simulation to derive interaction energies among all PCN

system components; 2) mapping of these values onto mesoscale parameters and subsequent simulations to determine system density distributions; and 3) simulations at finite-element levels to calculate the relative macroscopic properties (see Scheme 1). For the sake of brevity, the entire procedure is briefly reported. More detailed information about the recipe can be found in the Supporting Information.

The optimized chemical structure of montmorillonite (MMT) was taken from our previous work.[7] To model an MMT with a cation-exchange capacity (CEC) of approximately 92 meq/100 g (roughly corresponding to the CEC of the most commonly employed commercial products, e.g., Cloisite 20A and Cloisite 30B from Southern Clay Products, Inc., Gonzales, TX, USA), the basic cell was replicated three times in the *a* direction and twice in the *b* direction to obtain a supercell of dimensions $15.5\times17.9\times10$ Å, and four Al^{3+} ions were replaced by an equal number of Mg^{2+}. The resulting MMT model is described by the unit formula $(Al_{3.33}Mg_{0.67})Si_8O_{20}(OH)_4$–$Na_{0.67}$). The charges on the individual atoms were placed by following the charge scheme proposed by Cygan et al.,[8] and this finally yielded the overall neutral MMT cell model that was used in all subsequent simulations. In accordance with the idea of modeling Cloisite 20A and Cloisite 30B, 3D models of dimethyl- and trimethyldehydrogenated tallow quaternary ammonium chlorides ($M_2(C_{18})_2$ and M_3C_{18}, respectively; or quats) were built and optimized by using the Compass force field (FF).[9] The quat conformational search was carried out with our well-validated combined molecular mechanics/molecular dynamics simulated-annealing (MDSA) protocol.[7,10] These calculations were performed with the Materials Studio Discover module (v. 4.4, Accelrys, San Diego, CA, USA) and the Compass FF. The electrostatic charges for the geometrically optimized quat molecule were finally obtained by restrained electrostatic potential fitting,[11] and electrostatic potentials were produced by single-point quantum mechanical calculations at the Hartree–Fock level with a 6-31G* basis set. All ab initio calculations were carried out with the DMol^3 module,[12] as implemented in the Materials Studio modeling suite. To obtain a reasonable sampling of the Nylon 6 conformational space, ten different configurations of Nylon 6 chains at 298 K with a density of 1.12 g cm^{-3} were built. Each polymeric structure was then relaxed and subjected to the same MDSA protocol applied to model the quat molecule. Each final chain structure was assigned atomic charges according to the charge scheme proposed by Li and Goddard[13] (Scheme 1, step 1).

To generate atom-based pair correlation functions for the quats, 1 μs MD simulation at 300 K was performed with each single quat molecule in vacuo. Simple velocity rescaling was used to thermostat the temperature. The Verlet algorithm was employed to integrate the equations of motion, with a time step of 0.5 fs, the atomic valence interactions described with the OPLS all-atom force field,[14] and the intermolecular interactions were turned off. Atom coordinates were saved every 0.1 ps. The calculation was performed with the SingleMoleculeMD-Calculator of the Culgi software package.[15] To generate soft-core pair correlation functions for the quats, coarse-grained Brownian dynamics (BD) simulations were performed on each single quat molecule in vacuo with a repulsion parameter of 25 for all bead–bead interactions a_{ii}, a temperature value of 1 and a time step of 0.05. Each simulation lasted four million steps, and the bead coordinates were saved every 200 steps. The soft-core pair correlations were mapped onto atom-based pair correlation functions for the quats by overlapping the pair correlation functions obtained from the atomistically detailed model and the coarse-grained model, and judging the quality by visual inspection. If a positive agreement was obtained, then the MS bead number and architecture were established; otherwise, the number and type of bead were changed and the procedure repeated iteratively until a match was reached. As a final result, it was verified that the intramolecular size of an atomistically detailed model of the quat molecules had an optimal mapping if the coarse-grained molecule featured one head bead and one/two tails of each three beads (Scheme 1, steps 2–4).

The binding energies between the different components of each PCN system were obtained by performing constant volume/constant temperature (NVT) MD simulations. To reduce computational time, during each MD simulation, both montmorillonite layers were treated as rigid bodies by fixing all cell dimensions. All other atoms in the interlayer space (except the Na^+ ions of the MMT upper platelet) were allowed to move without any constraint. Each NVT simulation was run at 298 K for 500 ps with application of the Ewald summation method[16] for treating both van der Waals and electrostatic interactions. An integration time step of 1 fs and the Nosé thermostat[17] were also adopted (Scheme 1, step 5). The mesoscale nanocomposite model resulting from steps 2–4 contained four species of different beads: one for the polymer chain (P), two for the quat (H for the polar head and T for the apolar tail) and one to represent the MMT surface (M). The most complicated step in the entire proposed ansatz was proper mapping of the atomistic length scale to the mesoscale. For this purpose, a combinatorial approach was used to rescale the nonbonded interaction energies calculated at step 5 onto the repulsive DPD parameters a_{ij} between beads of different types (Scheme 1, step 6).

The generation of atom-based polymer density profiles required a complex MD-based procedure to carefully substitute the sodium ions with the corresponding quats, to insert the polymer chains and to obtain the correct equilibrium interlayer *d* spacing. Each corresponding system was in turn subjected to a final NVT annealing run, from which the lowest potential energy frame from the trajectory file was selected and used as starting configuration to perform a productive 300 ps NVT run with the Compass FF. Once the simulation was completed, 30 frames were extracted from the corresponding trajectory file, and on each one the density profile of the organic species (polymer and quat) within the interlayer space was calculated (Scheme 1, Step 7). To obtain a density profile of the polymer at the mesoscale level matching that obtained from the MD simulations of the previous step, several MS simulations were carried out with the mesoscopic bead–field (MBF) hybrid method. The quantity optimized was the so-called hybrid bead–field coupling parameter c_{jk}, where *j* is a field model and *k* a bead type, and its value is a measure of the free energy of interaction between the field and the bead. All calculations were performed with the MBFHybridCalculator of the Culgi software package[15] (Scheme 1, step 8). In similar fashion to the mapping of the quat (step 4), the density profile of the polymer obtained from the MD simulation with the density profile of the field model of the polymer as obtained from the MBF hybrid simulation was mapped by visual inspection. The optimal mapping was obtained by varying the hybrid bead–field coupling parameters.

The mesoscopic morphology of the PNC systems (Scheme 1, step 10) was generated by constructing a periodic system that consisted of clay platelets, cationic surfactant molecules (i.e., the quats) and the Nylon 6 polymer. Clay platelets and compatibiliser were represented as beads, and the polymer was chosen as the field model. Two to three square platelets, each one bead thick (ca. 7.4 Å), 15 beads long (11.1 nm), that is, the *x* and *y* edges of the simulation box, and an interlayer distance of five beads (ca. 3.7 nm) were employed. In agreement with the value obtained from the MD simulations the *d* spacing was 4.2 nm. The quat molecules consisted of one head bead and two tails of each three beads (i.e., $H(T_3)_2$) in the case of $M_2(C_{18})$ and of one head bead and one tail of three beads (i.e., HT_3) in the case of M_3C_{18}. The molecules were placed in a regular fashion, as far away as possible from each other, covering the platelets on both sites up to a cation exchange capacity of 1.0. Every molecule covered a surface area of about 139 Å^2 in agreement with the MD simulations (i.e., full coverage). For the bead–bead interaction parameters we used the values as obtained from step 6 and the beads did not bear a net charge. The reason we did not assign charges to the beads is that the effect of the charges is intrinsically already captured by the repulsion parameters computed at step 6. The Nylon 6 polymer consisted of a Gaussian chain of eight monomers corresponding to a length of about 6 nm. To get an overall system density of 3 we used a value of 4.6 for the Helfand compressibility parameter of the polymer field. For the bead–field coupling parameters we used the values as obtained at step 9. Initially, the polymer field model was equilibrated by means of dynamic density functional theory[18] by performing 2500 steps with a diffusion factor of 0.05 for the polymer field and all the beads fixed. In the second step we turned on bead diffusion, and a full hybrid MBF simulation was performed until the system was equilibrated. Since the system was still relatively small, equilibration was obtained after 50000 steps. The time step for the equation of motion of the beads was set to 0.02 and the temperature was set to 1. The diffusion factor was set to 0.01 for all bead

types, except for the clay beads, for which the value was set to 0. All calculations were performed with the MBFHybridCalculator of the Culgi software package.[15]

Finally, to calculate macroscopic properties of the investigated nanocomposite systems FEM simulations with fixed and variable grid were performed with the software Palmyra (v. 2.5, MatSim, Zürich, Switzerland). FE calculations were applied to analyze both platelet stacks and overall nanocomposite properties by using fixed and variable grids, respectively. In particular, Young's modulus was the macroscopic property of choice, since most of the industrial interest in these new materials lies in the mechanical performance. With regard to modeling the platelet stack, the hybrid density fields were imported into Palmyra after appropriate formatting of the MBF output files. Once imported, the density fields were divided into mesh elements, and the serial averaging system was selected to estimate the mechanical properties of the stack model. The properties of the quat molecules where chosen to match those of MMT and Nylon 6 for the cation heads and tails, respectively. Mechanical properties for pure silicate and polymer were taken from the available literature.[5,6a,19] Our MFB box resulted in $100\times100\times30$ Palmyra volume elements containing 300000 nodes and 1800000 tetrahedrons. After properties were assigned to each grid element, stack properties were calculated by using the method described for the variable grid mesh. Subsequently, overall nanocomposite properties were retrieved by defining a morphology similar to the corresponding TEM images,[5,6a] applying a variable grid mesh to the model and finally running Palmyra solver.

[1] For examples of recent reviews, see: a) *Polymer-Clay Nanocomposites* (Eds.: T. J. Pinnavaia, G. W. Beall), Wiley, New York, **2000**; b) S. S. Ray, M. Okamoto, *Prog. Polym. Sci.* **2003**, *28*, 1539–1641; c) Q. H. Zeng, A. B. Yu, G. Q. Lu, D. R. Paul, *J. Nanosci. Nanotechnol.* **2005**, *5*, 1574–1592; d) L. A. Utraki, *Clay-containing Polymeric Nanocomposites*, Rapra Tech. Ltd, London, **2004**; e) A. C. Balazs, T. Emrick and T. P. Russell, *Science* **2006**, *314*, 1107–1110; f) S. Pavlidou, C. D. Papaspyrides, *Prog. Polym. Sci.* **2008**, *33*, 1119–1198; g) D. R. Paul, L. M. Robeson, *Polymer* **2008**, *49*, 3187–3204, and references therein.

[2] a) E. P. Giannelis, *Adv. Mater.* **1996**, *8*, 29–35; b) P. C. LeBaron, Z. Wang, T. J. Pinnavaia, *Appl. Clay Sci.* **1999**, *15*, 11–29; c) M. Alexandre, P. Dubois, *Mater. Elektron. Mater. Sci. Eng.* **2000**, *28*, 1–63; d) D. Schmidt, D. Shah, E. P. Giannelis, *Curr. Opin. Solid State Mater. Sci.* **2002**, *6*, 205–212.

[3] Q. H. Zeng, A. B. Yu, G. Q. Lu, *Prog. Polym. Sci.* **2008**, *33*, 191–269.

[4] The MBF hybrid method is a new simulation technique that allows both beads and fields to be part of the same simulation. The beads and fields interact via a special free-energy coupling term (see the Supporting Information for more details).

[5] T. D. Fornes, D. L. Hunter, D. R. Paul, *Macromolecules* **2004**, *37*, 1793–1798.

[6] a) T. D. Fornes, D. R. Paul, *Polymer* **2003**, *44*, 3945–3961; b) A. Ranade, N. A. D'Souza, B. Gnade, A. Dharia, *J. Plast. Film Sheeting* **2003**, *19*, 271–285.

[7] a) M. Fermeglia, M. Ferrone, S. Pricl, *Fluid Phase Equilib.* **2003**, *212*, 315–329; b) M. Fermeglia, M. Ferrone, S. Pricl, *Mol. Simul.* **2004**, *30*, 289–300; c) R. Toth, A. Coslanich, M. Ferrone, M. Fermeglia, S. Pricl, S. Miertus, E. Chiellini, *Polymer* **2004**, *45*, 8075–8083; d) G. Scocchi, P. Posocco, M. Fermeglia, S. Pricl, *J. Phys. Chem. B* **2007**, *111*, 2143–2151.

[8] R. T. Cygan, J. J. Liang, A. G. Kalinichev, *J. Phys. Chem. B* **2004**, *108*, 1255–1266.

[9] a) H. Sun, *J. Phys. Chem. B* **1998**, *102*, 7338–7338–7364; b) H. Sun, P. Ren, J. R. Fried, *Comput. Theor. Polym. Sci.* **1998**, *8*, 229–246; c) D. Rigby, H. Sun, B. E. Eichinger, *Polym. Int.* **1998**, *45*, 311–330; d) S. W. Sun, H. Sun, *J. Phys. Chem. B* **2000**, *104*, 2477–2489.

[10] See for instance: a) M. Fermeglia, M. Ferrone, S. Pricl, *Bioorg. Med. Chem.* **2002**, *10*, 2471–2478; b) F. Felluga, G. Pitacco, E. Valentin, A. Coslanich, M. Fermeglia, M. Ferrone, S. Pricl, *Tetrahedron: Asymmetry* **2003**, *14*, 3385–3399; c) M. G. Mamolo, D. Zampieri, L. Vio, M. Fermeglia, M. Ferrone, S. Pricl, G. Scialino, E. Banfi, *Bioorg. Med. Chem.* **2005**, *13*, 3797–3809; d) A. Carta, G. Loriga, S. Piras, G. Paglietti, P. La Colla, G. Collu, M. A. Piano, R. Loddo, M. Ferrone, M. Fermeglia, S. Pricl, *Med. Chem.* **2006**, *2*, 577–589; e) G. Scialino, E. Banfi, D. Zampieri, M. G. Mamolo, L. Vio, M. Ferrone, M. Fermeglia, M. S. Paneni, S. Pricl, *J. Antimicrob. Chemother.* **2006**, *58*, 76–84; f) P. Posocco, M. Ferrone, M. Fermeglia, S. Pricl, *Macromolecules* **2007**, *40*, 2257–2266; g) D. Zampieri, M. G. Mamolo, L. Vio, E. Banfi, G. Scialino, M. Fermeglia, M. Ferrone, S. Pricl, *Bioorg. Med. Chem.* **2007**, *15*, 7444–7458; h) M. Mazzei, E. Nieddu, M. Mielea, A. Balbia, M. Ferrone, M. Fermeglia, M. T. Mazzei, S. Pricl, P. LaColla, F. Marongiu, C. Ibba and R. Loddo, *Bioorg. Med. Chem.* **2008**, *16*, 2591–2605, and references therein.

[11] C. I. Bayly, P. Cieplak, W. D. Cornell, P. A. Kollman, *J. Phys. Chem.* **1993**, *97*, 10269–10280.

[12] B. J. Delley, *J. Chem. Phys.* **1990**, *92*, 508–517.

[13] Y. Li, W. A. Goddard III, *Macromolecules* **2002**, *35*, 8440–8455.

[14] a) W. L. Jorgensen, D. S. Maxwell, J. Tirado-Rives, *J. Am. Chem. Soc.* **1996**, *118*, 11225–11236; b) D. S. Maxwell, J. Tirado-Rives, W. L. Jorgensen, *J. Comput. Chem.* **1995**, *16*, 984–1010.

[15] Culgi—The Chemistry Unified Language Interface, Version 2.2.0, Culgi BV, The Netherlands, **2007**.

[16] P. P. Ewald, *Ann. Phys. (Weinheim, Ger.)* **1921**, *64*, 253–287.

[17] S. Nosé, *Prog. Theor. Phys. Suppl.* **1991**, *103*, 1–46.

[18] J. G. E. M. Fraaije, *J. Chem. Phys.* **1993**, *99*, 9202–9212.

[19] G. W. Ehrenstein, *Polymeric Materials: Structure—Properties—Applications*, Hanser Gardner, Cincinnati, **2001**.

Received: April 15, 2009
Published online: July 2, 2009

